ISSN 1061-933X, Colloid Journal, 2016, Vol. 78, No. 2, pp. 210–219. © Pleiades Publishing, Ltd., 2016.
Original Russian Text © F.Kh. Urakaev, A.I. Bulavchenko, B.M. Uralbekov, I.A. Massalimov, B.B. Tatykayev, A.K. Bolatov, D.N. Dzharlykasimova, M.M. Burkitbayev, 2016, published in Kolloidnyi Zhurnal, 2016, Vol. 78, No. 2, pp. 193–202.

Mechanochemical Synthesis of Colloidal Sulfur Particles in the $Na_2S_2O_3$–$H_2(C_4H_4O_4)$–Na_2SO_3 System

F. Kh. Urakaev[a], A. I. Bulavchenko[b], B. M. Uralbekov[c], I. A. Massalimov[d], B. B. Tatykayev[c], A. K. Bolatov[c], D. N. Dzharlykasimova[c], and M. M. Burkitbayev[c]

[a] *Sobolev Institute of Geology and Mineralogy, Siberian Branch, Russian Academy of Sciences, pr. Akademika Koptyuga 3, Novosibirsk, 630090 Russia*

[b] *Nikolaev Institute of Inorganic Chemistry, Siberian Branch, Russian Academy of Sciences, pr. Akademika Lavrent'eva 3, Novosibirsk, 630090 Russia*

[c] *Al-Farabi Kazakh National University, pr. al-Farabi 71, Almaty, 050040 Kazakhstan*

[d] *Bashkortostan State University, ul. Zaki Validi 32, Ufa, Bashkortostan, 450074 Russia*

e-mail: urakaev@igm.nsc.ru

Received June 2, 2015

Abstract—Elemental sulfur nanoparticles (nanosulfur, S_n^0) have been obtained in a matrix consisting of sodium sulfite (diluent and a final reaction product) and succinic acid (catalyst) by mechanochemical syntheses via the reaction $Na_2S_2O_3 \cdot 5H_2O + H_2(C_4H_4O_4) + zNa_2SO_3 = (z + 1)Na_2SO_3 + H_2(C_4H_4O_4) + 5H_2O + S_n^0$, at $z = 19.6$. It has been shown that free nanodispersed sulfur can be obtained by dissolving the matrix in water. The prepared samples have been characterized using a set of physical and physicochemical methods.

DOI: 10.1134/S1061933X16020150

INTRODUCTION

Elemental sulfur is used in, e.g., production of sulfuric acid, varnishes, gunpowder, plastics, automobile tires, fertilizers, and antimicrobial agents; moreover, it is widely applied in agriculture, building, and other fields [1–4].

Sodium thiosulfate may be decomposed into sodium sulfite and sulfur. La Mer et al. were the first to obtain monodisperse spherical sulfur particles from acidified $Na_2S_2O_3$ solutions [5]. Their results have been used to develop a procedure for measuring nanoparticle size distribution based on the Mie [6] and Pecora [7] theories of light scattering.

In recent years, communications devoted to the study of sulfur nanoparticles (nanosulfur [8]) have been appearing at an increasing rate [8–50]. As a rule, common routine methods, including dynamic light scattering, scanning and transmission electron microscopy, X-ray diffraction analysis, and energy-dispersive X-ray spectroscopy, have been used in these works for studying the concentration, morphology, and structure of nanoparticles and nanostructured systems. Some specific methods used for studying sulfur nanoparticles should be especially noted; they include thermal analysis (thermogravimetry) [22, 23], atomic force microscopy [23], liquid chromatography [24], diffusion aerosol spectrometry using photoelectric counters of particles [17, 18], measurements of sorption properties [14] and ξ potential [22, 25], IR and Raman spectroscopy [13–15, 26], UV spectroscopy [8, 24, 27], and Rayleigh resonance scattering [15, 28].

Five main methods are available for producing nanodispersed sulfur. The first method consists in the acidification of a sodium thiosulfate solution with different acids [6, 16, 19] followed by stabilization of nanoparticles with surfactants [20, 29] or electrodeposition [30]. The second method is based on the reaction between sulfur and solutions of sulfides or hydroxides of ammonium and alkali or alkali-earth metals [13, 19, 21] (mechanical or ultrasonic activation of sulfur is necessary in this case) with the formation of corresponding solutions of polysulfides followed by varying the pH of the solutions and the use of corresponding surfactants. Modifications of these two methods include the use of water-in-oil microemulsions [13, 21, 31] or reaction between hydrogen sulfide and iron chelates [14]. The third method is sulfur sublimation followed by its homogeneous [17] or heterogeneous [18] nucleation, as well as its treatment with poly(ethylene glycol)s [28, 32] or cysteine [15]. The fourth method involves the modification of sulfur surface in surfactant solutions by successive mechanical and ultrasonic dispersing [33] (see also [34]). Finally, the fifth method represents the preparation of sulfur nanoparticles as components of composite materials [9, 26, 35–37].

In the majority of the cited works, synthesized sulfur nanoparticles had a spherical (α-S) or cylindrical (β-S) shape; however, they may be in the form of tubes

Initial reagents and parameters of mechanochemical synthesis of sulfur particles

Reagent	$Na_2S_2O_3 \cdot 5H_2O$ prepared from standard titer		$H_2(C_4H_4O_4)$ prepared from standard titer		Na_2SO_3, reagent grade	
Weighed portion, g	1.731		0.824		17.207	
ω, rpm	100	200	300	400	500	600
W, cm/s	130	260	390	520	650	780

[11], wires [12], and rods [28]. The spectrum of sizes of sulfur particles thus prepared is also wide (from a few nanometers to 1 μm). They can be prepared in a free state, as aqueous and nonaqueous dispersions, and as components of nanocomposites. The mechanism and kinetics of the formation and growth of sulfur particles in solutions have been studied in [38].

The diverse fields of nanodispersed sulfur application are based on its unique properties. Its bactericidal properties are employed in biotechnologies [4, 22, 23, 25], antiviral and antitumor activities are used in medicine [25, 32, , 34, 39, 40], pesticidal and fungicidal functions find application in agriculture [33, 41–43], its hydrophobicity is used in building [38, 44–46], and its electrochemical properties are employed in power engineering [9, 20, 26, 35–37, 47]. Sometimes, it is used in catalysis [10] and analytical chemistry [48]. Numerous allotropic modifications of sulfur are also widely used [49].

In this work, the method (which was described in our previous works [50, 51]) of system dilution with a side final product of the reaction

$$\begin{aligned} &Na_2S_2O_3 \cdot 5H_2O + yC_4H_6O_4 + zNa_2SO_3 \\ &= (z+1)Na_2SO_3 + yC_4H_6O_4 + 5H_2O + S_n^0. \end{aligned} \quad (1)$$

is, for the first time, proposed to be used for mechanochemical synthesis of nanodispersed sulfur.

Here, succinic acid $C_4H_6O_4$ and Na_2SO_3 play the roles of a catalyst and a diluent. Nanosulfur S_n^0 must be formed due to the decomposition of very unstable thiosulfuric acid according to the following scheme [16, 38, 52]:

$$\begin{aligned} &S_2O_3^{2-} + 2H^+ \rightleftarrows H_2S_2O_3 \rightarrow H_2SO_3 + S, \\ &S + S \rightleftarrows S_2 + S\ldots \rightleftarrows S_{n-1} + S \rightarrow S_n, \end{aligned} \quad (2)$$

where S_n is a nucleus of a critical size.

EXPERIMENTAL

Mechanical activation (MA) was performed in a Pulverisette planetary-type ball mill (Fritsch GmbH, Germany) with a cage rotation rate regulated in the range of 100–600 rpm and an apparatus made of hardened stainless still (cylinder volume was 500 cm^3 and the number of steel balls with a radius of 0.5 cm and a density of 7.8 g/cm^3 was 109). The stoichiometric coefficients in MA reaction (1) for the catalyst and diluent were $y = 1$ and $z = 19.6$, respectively.

The key parameter of the MA process in a planetary-type mill is relative rate W of interaction of grinding bodies, i.e., balls and cylinder walls [50]. Let R_1 and R_2 be the radii of the cage (distance between the axes of planetary movement, $R_1 = 6.2$ cm) and the cylinder ($R_2 = 5.0$ cm), respectively, and ω_1 and ω_2 be the angular rotation rates of the cage and the cylinder, respectively (in the used mill, they rotate in opposite directions at $|\omega_1| = |-\omega_2| = |\omega| = 2\pi\omega$, where ω is the rotation frequency). In this case, the geometric and kinematic factors are $\Gamma = R_1/R_2 = 6.2/5 = 1.24$ and $K = \omega_1/\omega_2 = -1$, respectively. Angle φ of ball detachment from the cylinder wall is determined by the relation $\cos\varphi = (1 + K)/\Gamma = 0$; hence, $\varphi = 90°$. In this case, W and its normal (W_n) and tangential (W_t) components at the moment of a collision of grinding bodies linearly depend on ω as follows:

$$\begin{aligned} |W| = W &= 2\pi\omega_1 R_2[(K+1)^2 + \Gamma^2 \\ &- 2\Gamma(K-1)\cos\varphi + (\Gamma+1)^2]^{0.5} \\ &= 2\pi\omega R_2[\Gamma^2 + (\Gamma+1)^2]^{0.5}, \\ W_n = |W|\sin\varphi = W,&\quad W_t = |W|\cos\varphi = 0. \end{aligned} \quad (3)$$

The characteristics and weighed portions of the initial reagents used for the mechanochemical synthesis nanodispersed sulfur via reaction (1) and the W values, which correspond to different rotation frequencies ω, as calculated by relations (3), are listed in the table.

In crystal-hydrate-containing systems, mechanochemical processes occur in the so-called mild conditions with release of H_2O [53, 54]. Therefore, to provide its removal from the reaction mixture, MA of the initial mixtures was performed without the packing strip of the mill cylinder at a balls-to-mixture weight ratio of 445.16/19.762 = 22.5. Note that, according to relation (1) and the data in the table, the yield of nanodispersed sulfur was expected to be 0.224 g.

A mixture was subjected to the mechanical treatment under conditions that excluded cylinder overheating in the following regime: initially, MA was performed at rotations rates of 140, 210, 280, and 350 rpm (14 min at each rate, 56 min in all); then, the cylinder was opened, inspected, and restacked; after that, the MA was carried out at 420, 490, 560, and 600 rpm (8, 4, 2, and 1 min, respectively, 15 min in all). After the experiment was completed (the total duration of MA

was 71 min), the product (18.207 g) was removed from the cylinder. Thus, the yield was $18.207/19.762 \approx 92\%$.

Free sulfur particles were obtained from the MA product by washing with water. The solubilities of possible products of MA in water have the following values: sodium thiosulfate, 70.1% (20°C); succinic acid, 5.8% (20°C); sodium sulfite, 20.82% (19.9°C); and sulfur is almost insoluble. The MA products used in an amount of $2.5 \times 4 = 10$ g were a fortiori soluble in $15 \times 4 = 60$ mL water placed into four centrifuge tubes. Thus, powder in an amount of 105 mg was obtained for analytical studies.

X-ray diffraction (XRD) analysis of the samples was carried out with a D8 ADVANCE diffractometer (Bruker AXS) using monochromatic radiation of copper. The measurements were performed in the following regime: X-ray tube voltage of 40 kV at a current of 40 mA, scanning step $2\theta = 0.02°$, and the time information acquisition at a point of 1 s. The XRD data were processed as described in [51] using the EVA.exe and PCPDFWIN softwares and the PDF-2 database, as well as by the method of the Reference Intensity Ratio.

The thermal analyses (thermogravimetric analysis (TGA) and differential scanning calorimetry (DSC)) were carried out in nitrogen with an STA 449 *F3* instrument (Netzsch, Germany) up to 1000°C at a heating rate of 10°/min.

Examination of the samples by scanning electron microscopy (SEM) was performed with a Quanta 3D 200i microscope (FEI, United States) operating at an accelerating voltage of 15 kV. The samples under examination were applied onto conducting carbon sticky tape.

Examination of the samples by transmission electron microscopy (TEM) was carried out with a JEM-1011 microscope (JEOL, Japan) equipped with a Morada digital camera (Olympus, Japan). A sample (10 mg) resulting from MA was placed into a tube with hexane (3 mL), and a droplet of the obtained suspension was applied onto a collodion-coated copper grid. Sulfur particles washed from side products of the synthesis were applied onto a grid from the suspension before the second decantation. Morphology and sizes of the particles were determined with a resolution below 5 nm at an accelerating voltage of 100 kV.

The sizes of sulfur nanoparticles were also determined by dynamic light scattering (DLS) at an angle of 90° using a 90Plus spectrometer (Brookhaven Inst., United States) equipped with a 35-mW solid-state laser (LaserMax, United States) operating at wavelength of 658 nm. Scattered photons were accumulated by a high-sensitivity detector based on an avalanche photodiode (Perkin Elmer). Hydrodynamic diameter d_z of particles averaged over scattered intensity was calculated under the assumption of their spherical shape as an average result of 100 measurements (ten series consisting of ten measurements each) by the Stokes–Einstein formula $d_z = kT/3\pi\eta D$. The values of viscosity η and refractive index of a dispersion were taken equal to those of the dispersion medium (water). Photon accumulation time during one measurement was 10 s, while the number of photons used for plotting the autocorrelation function was 10^5–10^6. In addition, the average light intensity scattered at an angle of 90° (static (Rayleigh) light scattering) was measured using the Debye Plot option as a number of photons (pulses) arriving at the detector per 1 s. The measurements were performed at 20 ± 0.1°C. The diffusion coefficient directly measured with the instrument is z-averaged (averaged over intensity). For a polydisperse system containing i number of components with different sizes, z-averaged diffusion coefficient D_z is calculated in terms of the monomodal analysis using the 90Plus software as follows:

$$D_z = \frac{\sum_i I_i D_i}{\sum_i I_i}.$$

Expressing D_i via corresponding diameters and taking into account that intensity I of light scattered by particles is, according to the Rayleigh theory, proportional to their number concentration N_i and six-powered diameter d, we obtain

$$d_z = \frac{\sum_i I_i}{\sum_i \frac{I_i}{d_i}} = \frac{\sum_i N_i d_i^6}{\sum_i N_i d_i^5}.$$

As follows from the derived expression, in the DLS method, the contribution from large particles of a polydisperse system to the d_z value may appear to be determining. More "recognized" number-average diameter d_n is a derived quantity: $d_n = \Sigma Nd/\Sigma N$.

The error in the calculation of d_n may be substantial. Note that the "reference" method of particle size determination from TEM data enables one to directly find only d_n. Other distributions are also derived parameters, which are calculated with a much larger error. Therefore, the TEM and DLS data may be compared only within the framework of equivalent averagings. For monodisperse samples, $d_n = d_z$, while, for polydisperse ones, $d_n < d_z$. In the monomodal analysis, which implies the existence of a single mode, the autocorrelation function is processed by the cumulant method using the 90Plus software. The average hydrodynamic diameter and polydispersity are determined from the first and second cumulants, respectively; therewith, the nanoparticle size distribution is approximated by a lognormal dependence.

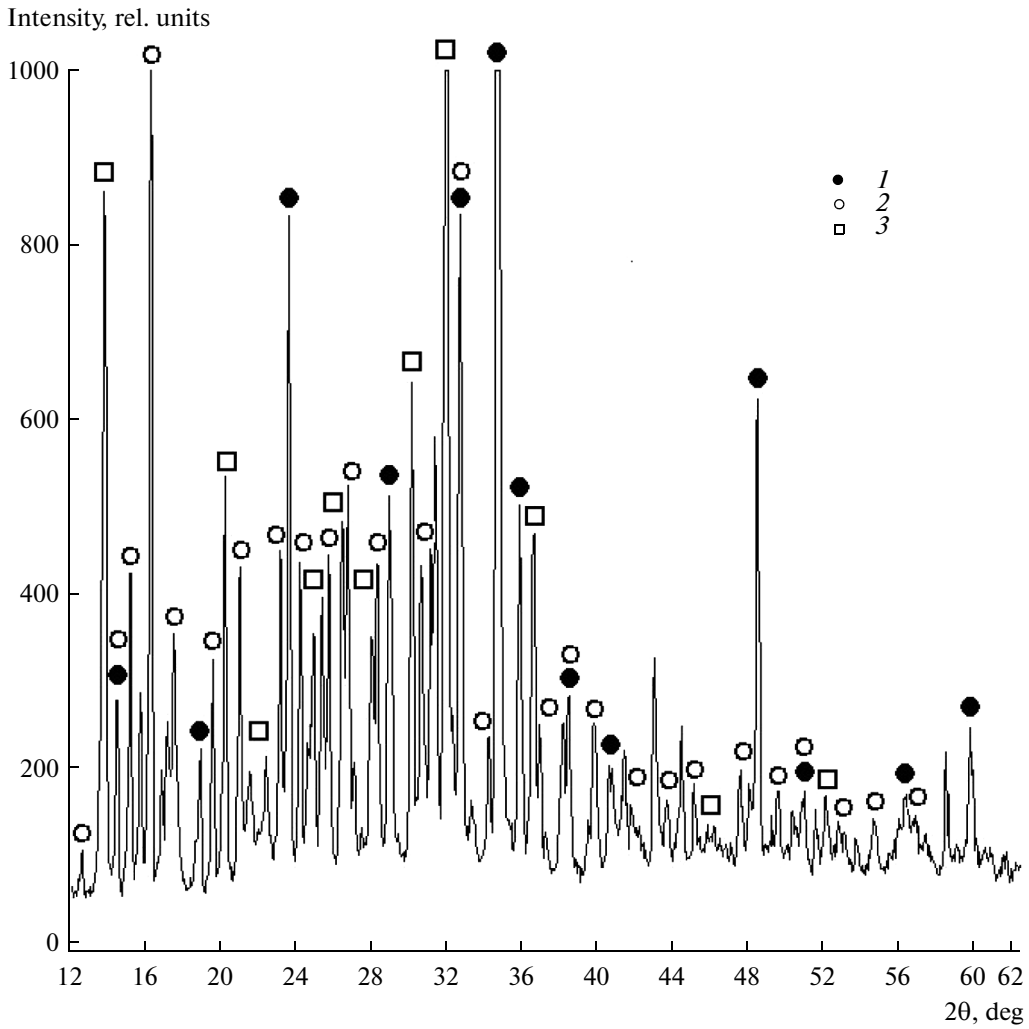

Fig. 1. Diffraction pattern of a mixture (2.1 g; $y = 1$, $z = 2$) of reagents for reaction (1) prepared in an agate mortar of the Pulverisette mill: (*1*) Na_2SO_3, (*2*) $Na_2S_2O_3 \cdot 5H_2O$, and (*3*) $C_4H_6O_4$.

RESULTS AND DISCUSSION

X-ray Diffraction and Thermal Analyses

Initially, we tried to carry out reaction (1) an a Pulverisette homogenizer/grinder (Fritsch GmbH, Germany) equipped with an agate mortar and a ball 9.2 and 7.1 cm in diameter, respectively, at $y = 1$ and $z = 2$ (mixture weight was 2.1 g). The XRD data are illustrated in Fig. 1. It can be seen that the reaction has not been realized, because the lines assigned to the initial reagents and, possibly, succinic acid derivatives (anhydrous and hydrated sodium succinate) are predominantly observed.

Figure 2 depicts the diffraction patter of the products of MA of the initial mixture in a Pulverisette 6 planetary-type mill. It can be seen that the lines attributed to sodium sulfite playing the role of a diluent prevail because of the high dilution parameter. At the same time, the low content of, e.g., sulfur, whose theoretical yield from reaction (1) is as low as 0.224 g (1.13 wt % in the MA product), makes it impossible to correctly identify the presence of its phase from the XRD data.

The XRD data on a powder obtained from an MA product by treatment with water are presented in Fig. 3a. The processing of these data have shown that this sample represents monophase sulfur (α-S) with size of coherent-scattering regions $L \approx 75$ nm and the following parameters of unit cell (Å) $a = 10.4430 \pm 0.0030$, $b = 12.8499 \pm 0.0034$, $c = 24.4427 \pm 0.0060$, which have appeared to be somewhat larger than $a = 10.4370$, $b = 12.845$, $c = 24.369$ Å characteristic of reference sulfur (Fig. 3b).

Moreover, comparative thermal analysis was performed for samples of ordinary sulfur (extrapure grade, Technical Certificate TU 6-09-2546-77) and the same powder of nanodispersed sulfur (Fig. 4, curves *1*, *2*, respectively). The obtained TGA/DSC curves suggest that sulfur nanoparticles have higher

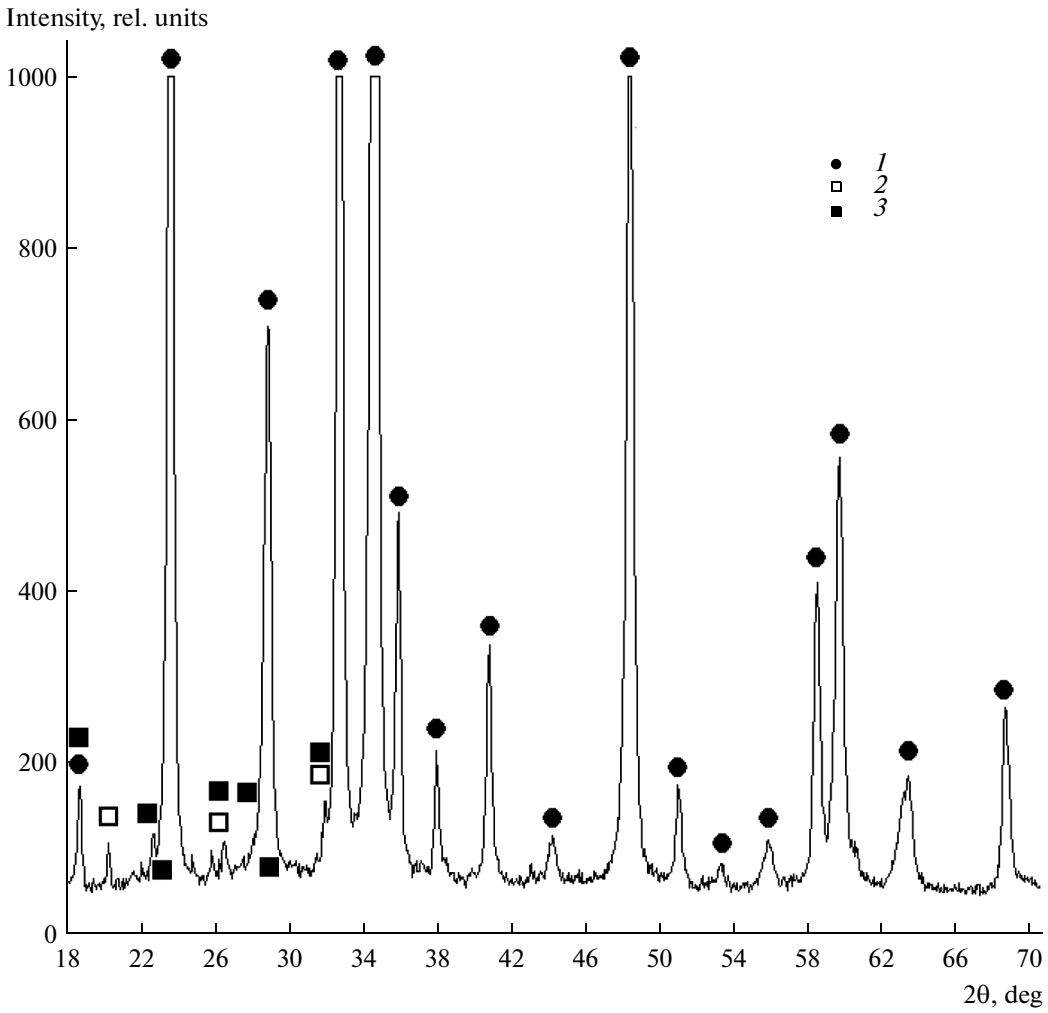

Fig. 2. Diffraction pattern of a reaction mixture (19.134 g; $y = 1$, $z = 19.6$) after MA in a Pulverisette 6 mill: (*1*) Na_2SO_3, (*2*) $C_4H_6O_4$ (?), and (*3*) S (?).

temperatures of the $\alpha \rightarrow \beta$ transformation and complete evaporation, but lower temperatures of the onset of evaporation and polymerization at the same melting temperatures of these two samples. It is worth especially noting that the magnitudes of the thermal effects of melting and polymerization for nanodispersed sulfur are markedly lower than those for ordinary sulfur are.

Measurements of Sulfur Nanoparticle Sizes

Analysis of SEM micrographs (Fig. 5) has confirmed the sulfur nanoparticles sizes calculated from the XRD data (Fig. 3) for a mechanically activated sample (Fig. 5a). Because of the close atomic masses of the components, the SEM images are insufficiently contrasted; however, their detailed examination leads us to conclude that the issue is particles with sizes of nearly 100 nm. Another picture is observed for sulfur particles resulting from the treatment of a mechanically activated sample with water and deposited onto a substrate from a suspension before the second decantation (Fig. 5b). In this case, the particle sizes are substantially larger than 100 nm; however, according to the XRD data, the size of their coherent-scattering regions is $L \approx 75$ nm (Fig. 3a).

The TEM images of a mechanically activated sample and sulfur particles isolated from it are shown in Fig. 6. As can be seen from Fig. 6a, the sizes of sulfur particles in the mechanically activated sample are 20–80 nm, while their morphology agrees with that described in the literature (see, e.g., [55]). The sizes (as large as 300 nm) and morphology of washed sulfur particles (Fig. 6b) differ from those observed for the mechanically activated sample, seemingly because of recrystallization processes (seeded growth and the development of the spherical shape at the expense of smaller particles) during the preparation of particles.

Information on the behavior of sulfur nanoparticles after the dissolution of the mechanically activated sample in water (Fig. 7) has been obtained by DLS.

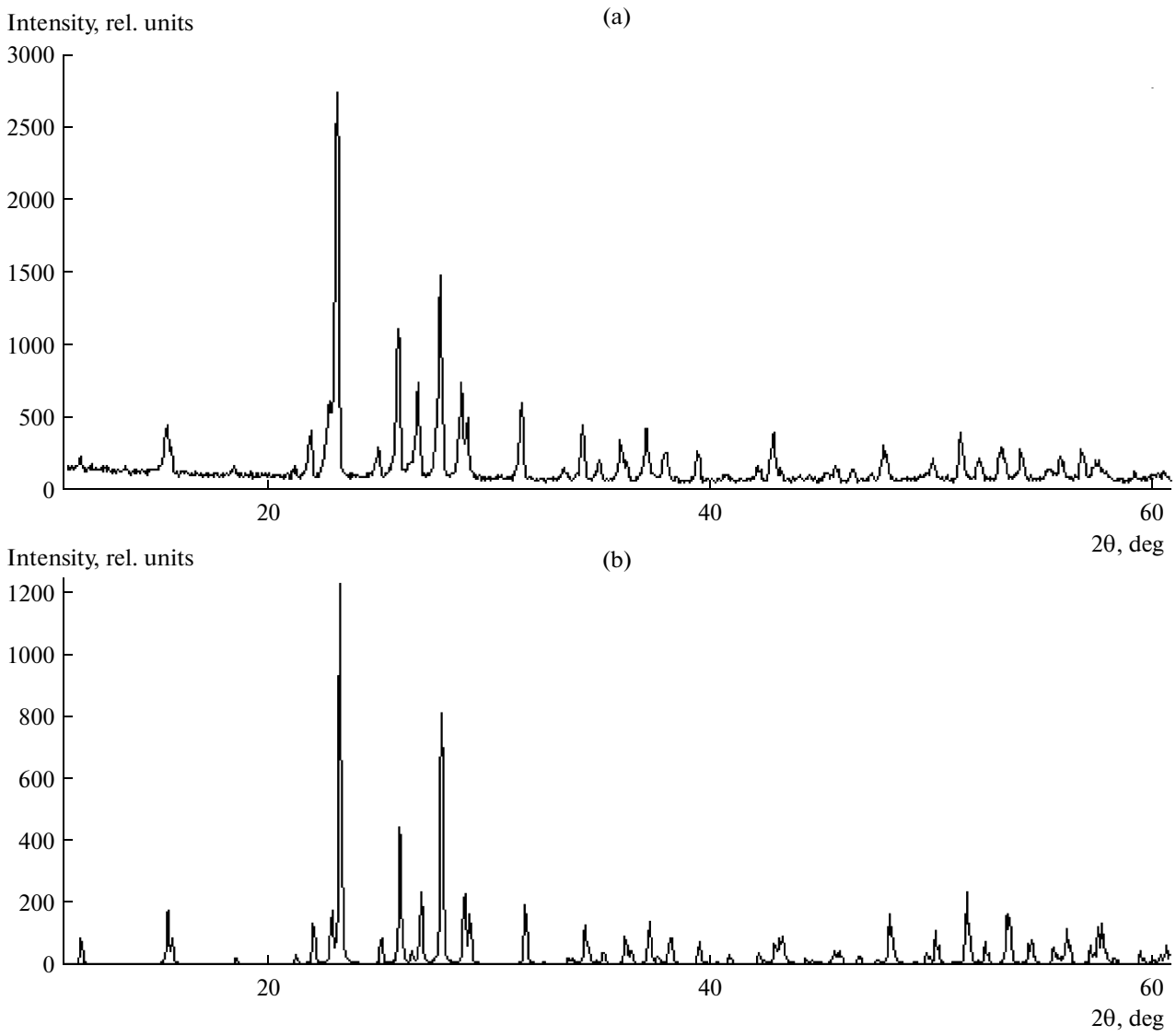

Fig. 3. Diffraction patterns of (a) sulfur washed out of a mechanically activated sample and (b) reference sulfur (PDF 83-2285).

The data presented in Fig. 7a show that the effective hydrodynamic diameter of particles immediately after the sample dissolution (within the initial 24 h) does not change significantly, probably because the solution contains succinic acid anions, which play the role of a surfactant stabilizing the sulfur nanodispersion. Then, the size of the nanoparticles begins to dramatically increase, and, in 3 days, after the particles reach sizes of several microns, their hydrodynamic diameters begin to strongly decrease. In addition, the obtained dispersion was heated to 40 and 70°C. During the initial 2 h of exposure at these temperatures, the hydrodynamic diameter of the particles did not increase noticeably as well.

As has been mentioned above, the intensity of the Rayleigh light scattering is proportional to the product of nanoparticle concentration and six-powered particle diameter. Therefore, at the initial stage, the experimental time dependence of the scattered light intensity has a more complex pattern (Fig. 7b), while a drastic decrease in the intensity is observed in 24 h due to partial sedimentation of the particles. The obtained data lead us to conclude that the obtained sulfur hydrosol is relatively stable during the initial 24 h, which must be taken into account when using it in practice. Coagulation then begins in the system, and the sol loses its stability with respect to aggregation and, judging by the abrupt fall in the scattered light intensity, to sedimentation as well.

The DLS and TEM data have also be compared (Fig. 8). Comparison has been performed using the number-average values of the particle diameter. It can be seen from the figure that sulfur particles in the sol have smaller sizes than those after the deposition onto

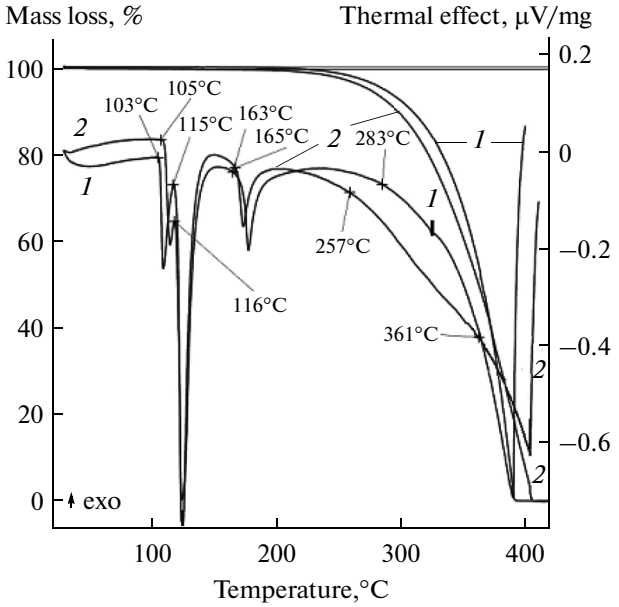

Fig. 4. TGA/DSC curves for (*1*) ordinary sulfur and (*2*) sulfur particles washed out of a mechanically activated sample.

the substrate. Seemingly, when the samples are prepared for TEM examination, sulfur nanoparticles additionally grow, most likely with involvement of gravitational forces during the first centrifugation at 7000 rpm.

CONCLUSIONS

A short review of the literature data on the properties and the methods for investigation and production of sulfur nanoparticles (nanosulfur) has been presented. A method has, for the first time, been proposed for mechanochemical synthesis of nanodispersed sulfur in a sodium thiosulfate pentahydrate/succinic acid system involving dilution with a water-soluble final reaction product, sodium sulfite. Using X-ray diffraction and thermal analyses, it has been shown that washing of mechanical activation product with water leads to the isolation of finely dispersed sulfur particles with a size of coherent-scattering regions equal to 75 nm and thermal properties somewhat different from those of ordinary sulfur.

Electron microscopy and dynamic light scattering have been employed to determine the sizes of sulfur particles in the product of mechanical activation (below 100 nm) and in the free state (as large as 300

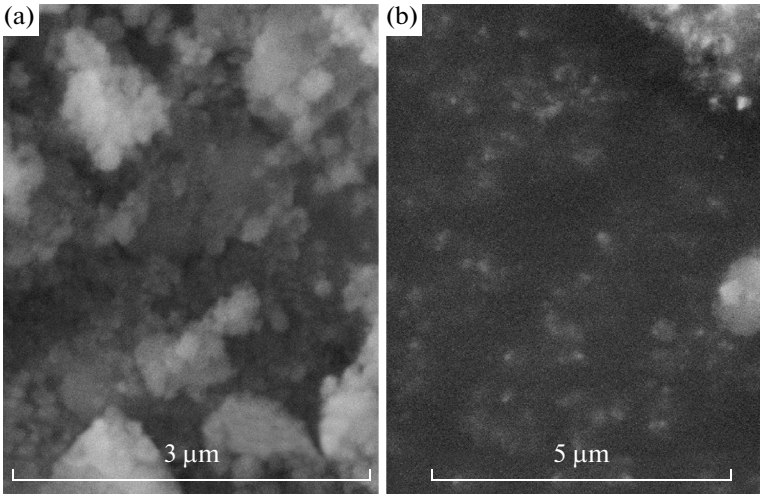

Fig. 5. SEM images of (a) a mechanically activated sample and (b) sulfur particles washed out of this sample.

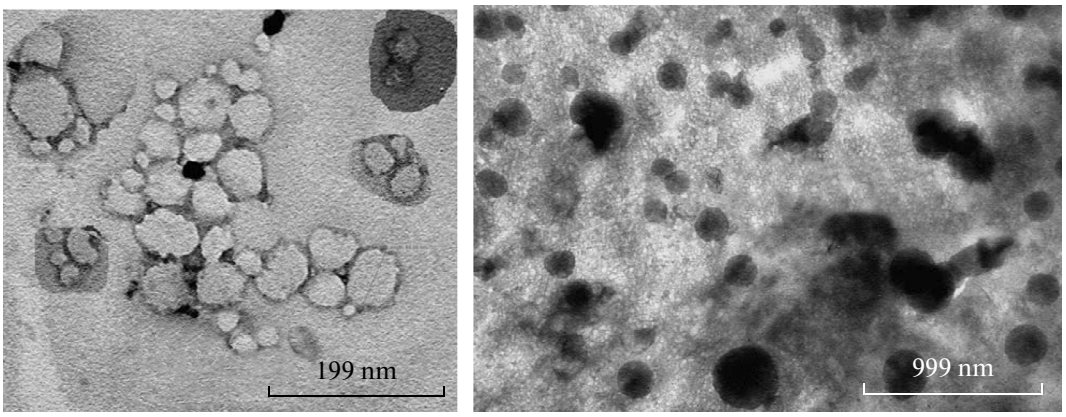

Fig. 6. TEM images of (a) mechanically activated sample assembles from different regions of visual field at 100000× magnification and sulfur particles washed out of this sample (200000×) (b).

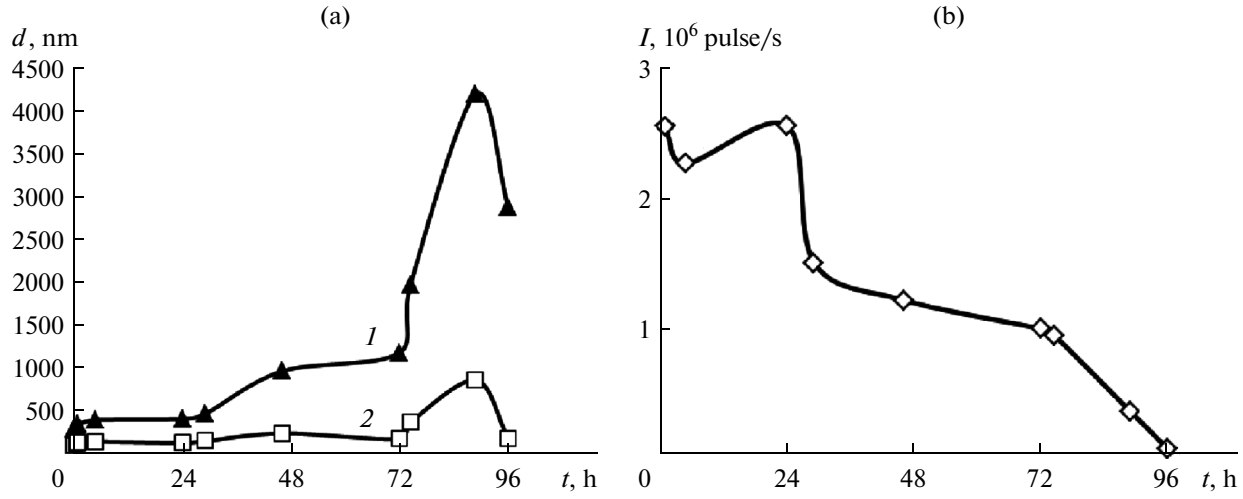

Fig. 7. Panel (a): time dependences of (*1*) d_z and (*2*) d_n for particles of sulfur sol obtained by dissolving a mechanically activated sample in water and panel (b): time dependence of intensity I of light scattered by this sol.

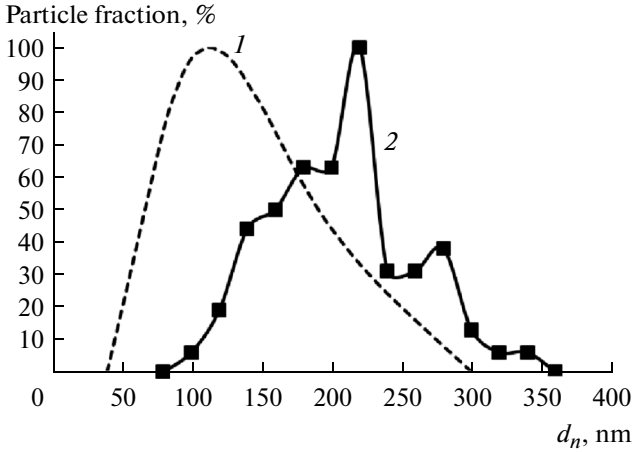

Fig. 8. Sulfur particle size distributions obtained using (*1*) DLS and (*2*) TEM. Dependences have been normalized by 100% with respect to the maximum point. Experiments were performed 30 min after the sulfur sol was prepared.

nm) and to establish that, during the preparation of free sulfur, its particles acquire a spherical shape.

ACKNOWLEDGMENTS

We are grateful to V.I. Antonyuk, N.R. Guseinov, E.E. Dil'mukhambetov, Zhanar Nurakhmetova, and Zhandos Ukibaev for their help in performing analytical experiments. This work was supported by the "Program-Purpose Financing of the Republic of Kazakhstan" (contract no. 586 of April 7, 2015) and the Russian Foundation for Basic Research (project no. 15-05-03980A).

REFERENCES

1. Kutney, G., *Sulfur: History, Technology, Applications & Industry,* Toronto: ChemTec, 2013.

2. Sangalov, Yu.A., Karchevskii, S.G., and Telyashev, R.G., *Elementnaya sera. Sostoyanie problemy i napravleniya razvitiya. Sera, vysokosernistye soedineniya i kompozitsii na ikh osnove* (Elemental Sulfur. The State of Problem and Development Lines. Sulfur, High-Sulfur Compounds and Related Compositions), Ufa: GUP INKhP Resp. Bashkortostan, 2010.
3. Schmid, G., *Clusters and Colloids: From Theory to Applications*, New York: Wiley, 1994.
4. Liu, W.-T., *J. Biosci. Bioeng.*, 2006, vol. 102, p. 1.
5. La Mer, V.K., *Ind. Eng. Chem.*, 1952, vol. 44, p. 1270.
6. Barnes, M.D., Kenyon, A.S., Zaiser, E.M., and La Mer, V.K., *J. Colloid Sci.*, 1947, vol. 2, p. 349.
7. Berne, B.J. and Pecora, R., *Dynamic Light Scattering with Applications to Chemistry, Biology and Physics*, New York: Dover, 2000.
8. Kumar, R., Nair, K.K., Alam, M.I., Gogoi, R., Singh, P.K., Srivastava, C., Yadav, S., Gopal, M., Chaudhary, S.R., Pradhan, S., and Goswami, A., *Curr. Sci.*, 2011, vol. 100, p. 1542.
9. Zheng, W., Liu, Y.W., Hu, X.G., and Zhang, C.F., *Electrochim. Acta*, 2006, vol. 51, p. 1330.
10. Lan, Y., Deng, B., Kim, C., Thornton, E.C., and Xu, H., *Environ. Sci. Technol.*, 2005, vol. 39, p. 2087.
11. Bezverkhyy, I., Afanasiev, P., Marhic, C., and Danot, M., *Chem. Mater.*, 2003, vol. 15, p. 2119.
12. Santiago, P., Carvajal, E., Mendoza, D.M., and Rendon, L., *Microsc. Microanal.*, 2006, vol. 12, no. S02, p. 690.
13. Guo, Y., Zhao, J., Yang, S., Yu, K., Wang, Z., and Zhang, H., *Powder Technol.*, 2006, vol. 162, p. 83.
14. Deshpande, A.S., Khomane, R.B., Vaidya, B.K., Joshi, R.M., Harle, A.S., and Kulkarni, B.D., *Nanoscale Res. Lett.*, 2008, vol. 3, p. 221.
15. Xie, X.-Y., Zheng, W.-J., Bai, Y., and Liu, J., *Mater. Lett.*, 2009, vol. 63, p. 1374.
16. Urakaev, F.Kh., Bazarov, L.Sh., Meshcheryakov, I.N., Feklistov, V.V., Drebushchak, T.N., Savintsev, Yu.P., Gordeeva, V.I., and Shevchenko, V.S., *Colloid J.*, 1999, vol. 61, p. 647.
17. Valiulin, S.V., Karasev, V.V., Vosel', S.V., and Onishchuk, A.A., *Colloid J.*, 2013, vol. 75, p. 14.
18. Valiulin, S.V., Vosel', S.V., Karasev, V.V., Onishchuk, A.A., Baklanov, A.M., and Purtov, P.A., *Colloid J.*, 2014, vol. 76, p. 271.
19. Massalimov, I.A., Khusainov, A.N., Zainitdinova, R.M., Musavirova, L.R., Zaripova, L.R., and Mustafin, A.G., *Russ. J. Appl. Chem.*, 2014, vol. 87, p. 700.
20. Suleiman, M., Ali, A.A., Hussein, A., Hammouti, B., Hadda, T.B., and Warad, I., *J. Mater. Environ. Sci.*, 2013, vol. 4, p. 1029.
21. Choudhury, S. and Goswami, A., *J. Appl. Microbiol.*, 2013, vol. 114, p. 1.
22. Choudhury, S., Mandal, A., Chakravorty, D., Gopal, M., and Goswami, A., *J. Nanopart. Res.*, 2013, vol. 15.
23. Choudhury, S., Ghosh, M., Mandal, A., Chakravorty, D., Pal, M., Pradhan, S., and Goswami, A., *Appl. Microbiol. Biotechnol.*, 2011, vol. 90, p. 733.
24. Nair, K.K., Siddiqi, W.A., Kumar, R., Niwas, R., Gogoi, R., Srivastava, C., and Gopal, M., *J. Sep. Sci.,* 2014, vol. 37, p. 1126.
25. Choudhury, S., Mandal, A., Ghosh, M., Basu, S., Chakravorty, D., and Goswami, A., *Appl. Microbiol. Biotechnol.*, 2013, vol. 97, p. 5965.
26. Wang, J.-Z., Lu, L., Choucair, M., Stride, J.A., Xu, X., and Liu, H.-K., *J. Power Sources,* 2011, vol. 196, p. 7030.
27. Chaudhuri, R.G. and Paria, S., *J. Colloid Interface Sci.*, 2011, vol. 354, p. 563.
28. Xie, X.-F., Li, L.-Y., Zheng, P.-S., Zheng, W.-J., Bai, Y., Cheng, T.-F., and Liu, J., *Mater. Res. Bull.*, 2012, vol. 47, p. 3665.
29. Chaudhuri, R.G. and Paria, S., *J. Colloid Interface Sci.*, 2010, vol. 343, p. 439.
30. Shamsipur, M., Pourmortazavi, S.M., Roushani, M., Kohsari, I., and Hajimirsadeghi, S.S., *Microkhim. Acta*, 2011, vol. 173, p. 445.
31. Choudhury, S., Dey, K.K., Bera, S., and Goswami, A., *J. Exp. Nanosci.*, 2013, vol. 8, p. 267.
32. Choudhury, S., Roy, S., Goswami, A., and Basu, S., *J. Antimicrob. Chemother.*, 2012, vol. 67, p. 1134.
33. Turganbay, S., Aidarova, S.B., Bekturganova, N.E., Alimbekova, G.K., Musabekov, K.B., and Kumargalieva, S.S., *Adv. Mater. Res.*, 2013, vols. 785—786, p. 475.
34. An, Y.-L., Nie, F., Wang, Z.-Y., and Zhang, D.-S., *Int. J. Nanomed.*, 2011, vol. 6, p. 3187.
35. Rao, M., Song, X., and Cairns, E.J., *J. Power Sources*, 2012, vol. 205, p. 474.
36. Zhang, S.S., *J. Power Sources*, 2013, vol. 231, p. 153.
37. Zhang, Y., Zhao, Y., Konarov, A., Gosselink, D., Soboleski, H.G., and Chen, P., *J. Power Sources*, 2013, vol. 241, p. 517.
38. Urakaev, F.Kh., *Int. J. Comput. Mater. Sci. Surf. Eng.,* 2011, vol. 4, p. 69.
39. Porras, I., *Appl. Radiat. Isotopes*, 2011, vol. 69, p. 1838.
40. Choudhury, S., Basu, A., Nag, T., Sengupta, K., Bhowmik, M., and Goswami, A., *Environ. Toxicol. Pharmacol.*, 2013, vol. 36, p. 675.
41. Choudhury, S., Ghosh, M., and Goswami, A., *Curr. Microbiol.*, 2012, vol. 65, p. 91.
42. Rao, K.J. and Paria, S., *RSC Adv.*, 2013, vol. 3, p. 10471.
43. Massalimov, I.A., Medvedev, U.A., Zaynitdinova, R.M., Mufazalova, N.A., and Mustafin, A.G., *Nanotechnol. Nanosci.*, 2012, vol. 3, p. 55.
44. Elesin, M.A., Pavlov, A.V., Berdov, G.I., Mashkin, N.A., and Oglezneva, I.M., *Russ. J. Appl. Chem.*, 2002, vol. 75, p. 883.
45. Beben, D. and Manko, Z., *Constr. Build. Mater.*, 2011, vol. 25, p. 282.
46. Massalimov, I.A., Yanakhmetov, M.R., Chuykin, A.E., and Mustafin, A.G., *Study Civil Eng. Architect.*, 2013, vol. 2, p. 19.
47. Cañas, N.A., Hirose, K., Pascucci, B., Wagner, N., Friedrich, K.A., and Hiesgen, R., *Electrochim. Acta*, 2013, vol. 97, p. 42.

48. Ghanemi, K., Nikpour, Y., Omidvar, O., and Maryamabadi, A., *Talanta*, 2011, vol. 85, p. 763.
49. Urakaev, F.Kh., *Combust. Sci. Technol.*, 2013, vol. 185, p. 1281.
50. Urakaev, F.Kh., *Int. J. Comput. Mater. Sci. Surf. Eng.*, 2011, vol. 4, p. 347.
51. Urakaev, F.Kh., Burkitbaev, M.M., Tatykaev, B.B., and Uralbekov, B.M., *Colloid J.*, 2015, vol. 77, p. 641.
52. Urakaev, F.Kh., Drebushchak, T.N., Savintsev, Yu.P., and Drebushchak, V.A., *Mendeleev Commun.*, 2003, vol. 13, p. 37.
53. Avvakumov, E., Senna, M., and Kosova, N., *Soft Mechanochemical Synthesis: A Basis for New Chemical Technologies*, Boston: Kluwer Academic, 2001.
54. Billik P., Čaplovičová M. *Adv. Nanotechnol.*, 2012, vol. 8, p. 111.
55. Suleiman, M., Al-Masri, M., Al Ali, A., Aref, D., Hussein, A., Saadeddin, I., and Warad, I., *J. Mater. Environ. Sci.*, 2015, vol. 6, p. 513.

Translated by A. Kirilin